Front. Earth Sci. 2020, 14(1): 221–235
https://doi.org/10.1007/s11707-019-0767-7

RESEARCH ARTICLE

# Spatiotemporal dynamics of the vegetation in Ningxia, China using MODIS imagery

**Yi HE[1,2,3], Haowen YAN (✉)[1,2,3], Lei MA[1,2,3], Lifeng ZHANG[1,2,3], Lisha QIU[1,2,3], Shuwen YANG[1,2,3]**

1 Faculty of Geomatics, Lanzhou Jiaotong University, Lanzhou 730700, China
2 National-Local Joint Engineering Research Center of Technologies and Applications for National Geographic State Monitoring, Lanzhou Jiaotong University, Lanzhou 730700, China
3 Gansu Provincial Engineering Laboratory for National Geographic State Monitoring, Lanzhou Jiaotong University, Lanzhou 730700, China



**Abstract** The vegetation in the Ningxia Hui Autonomous Region (henceforth, Ningxia) of north-western China plays an important role in guarding regional ecological safety and sustainable development. However, it is unclear how climate affects vegetation growth in terms of seasonality and various vegetation types in Ningxia. Based on remote sensing vegetation index from 2001 to 2016, climatic parameters, and the Chinese vegetation type data, this article examines the spatiotemporal effects of climate parameters on vegetation. The relative importance to variability in the normalized difference vegetation index (NDVI) for different seasons and various vegetated types is also determined. The results demonstrate that the vegetation increased from 2001 to 2016 in Ningxia. The rate of NDVI increase was fastest in summer and slowest in spring. Areas with significant increases in vegetation occurred primarily in the southern mountain, Liupan Mountain, and central arid areas. Degraded vegetation occurred in the Yellow River irrigation area with intense human activity influence. The vegetation in most areas of Ningxia will continue to increase in the future. The sensitivity of vegetation to temperature, precipitation, sunshine duration, and wind velocity showed significantly seasonal variability. Sunshine duration and wind velocity were important climatic factors affecting vegetation growth in Ningxia. However, the impact of summer precipitation variation on summer NDVI (SMN) demonstrated a time lag effect. The impact of climate variation on vegetation was distinct among various vegetation types. Moreover, the spatial pattern of vegetation in Ningxia was also impacted by human activities.

**Keywords** spatiotemporal patterns, vegetation NDVI, climatic parameter, Hurst exponent, Ningxia

Received November 7, 2018; accepted June 2, 2019

E-mail: heyi8738@163.com

## 1 Introduction

Global climate has undergone substantial changes that significantly affect human lives, natural environments, and socio-economic development. Vegetation can reflect climate change and has been used to detect changes in the water, soil and atmosphere (Gerten et al., 2004; Guo et al., 2014; Lei et al., 2014; Mao et al., 2015; Nair et al., 2017). Previous research has shown the relations between vegetation and climate exhibiting specific characteristics in different regions, e.g., the correlation of vegetation to climate parameters was very strong in one place with one certain time, but weak in other locations at different times (Zhao et al., 2011; Wang et al., 2015; Zhang and Wang, 2015). Therefore, it is clear that the effect of climate variation on vegetation is spatiotemporally correlated in different geographic regions. Furthermore, it needs to be further explored. Vegetation is an important part of the ecosystem and responds to climate variation in north-western China and Central Eurasia. These regions are characterized by slight precipitation and thin vegetation, and have a high risk of desertification (Jamali et al., 2014). Ningxia Hui Autonomous Region (henceforth, Ningxia) in north-western China is a typical arid region characterized by a fragile ecological environment. Vegetation change in Ningxia can guard the regional ecological security of the north-western China. Therefore, considerable research focused on vegetation change in Ningxia (e.g., Jin et al., 2007; Du and Tian, 2012; Zong and Wang, 2014).

The NDVI is largely applied for vegetation dynamic monitoring that is affected by climatic changes (Mao et al., 2012). Using NDVI, researchers have achieved significant advancements in the field (Hu et al., 2011; Zhang et al., 2013a; Xu et al., 2016). Research in the field included following: Chen et al. (2007) used GIMMS NDVI data to analyze the average vegetation coverage in each geographical unit from 1982 to 2004 and establish statistical

relations among precipitation and temperature. Jin et al. (2007) analyzed the variability trends of NDVI by utilizing GIMMS and MODIS data in Ningxia during 1982–2004. Du and Tian (2012) calculated the vegetation coverage of this region based on the 10-day Small Programmable Object Technology-Vegetation (SPOT-VGT) NDVI (1 km × 1 km) data from 1999 to 2009 and analyzed their variations. Zong and Wang (2014) used NDVI data (500 m × 500 m) to obtain the seasonal changes in vegetation as well as the relationship with temperature, precipitation, and sunshine duration from 2001 to 2011. Hua et al. (2017) investigated the relations between vegetation and drought in Northern China (including the Ningxia region) using the NDVI3g and SPEI. The influence of climate variation on vegetation varied with vegetation type (Xu et al., 2017). The main climatic factors affecting vegetation growth included temperature, accumulated precipitation, and solar duration (Nemani, 2003; Ghosh, 2018); wind velocity also affected vegetation coverage and caused sand and salt dust events (Sun et al., 2018; Yao, 2018). Ningxia is situated on the leading edge of the Tengger, Mu Us, and Ulan Buh deserts. It is subject to dust storms and channels of sand intrude into the Beijing-Tianjin-Hebei region (Du and Tian, 2011). Wind velocity is likewise a major indicator of vegetation growth in this region. There are limited studies on relationships between different vegetation types and climate parameters in Ningxia. Additionally, it is difficult to find studies of the changes of NDVI and the influence of climatic parameters on vegetation in the recent two decades. Efforts for studying the relative role of different climatic parameters in vegetation response had limited success. Therefore, this study analyzed change trends of vegetation seasonally and assessed the response of vegetation to various climatic parameters.

The aim of this article is to detect the spatiotemporal dynamics and sustainability of vegetation seasonally and determine the relative importance ranking of temperature, precipitation, sunshine duration, and wind velocity to seasonal NDVI and vegetation types. Based on the TERRA/MODIS NDVI data (250 m × 250 m) during 2001–2016, in conjunction with climate parameters, as well as the Chinese vegetation type data at a scale of 1:1,000,000, this article studied the spatiotemporal influence of climatic parameters on vegetation in Ningxia. It is crucial to understand the regional ecological environment and promote the ecological sustainable development.

## 2 Data and methods

### 2.1 Study area

Ningxia is situated in the middle-upper stream of the Yellow River. This region is located in the north-west of the Loess Plateau. The total area is $5.18 \times 10^4$ km$^2$ (Fig. 1(a)). The Yinchuan Plain is in the north of Ningxia. The Yellow River brings abundant water to the Yinchuan Plain, turning it into the most prosperous area of this region (Chen et al., 2007). The innermost region of Ningxia includes the hilly mountain and mountain basin, which exhibits typical grassland desertification. The climate is dry and the vegetation is sparse. This region includes part of the Loess Plateau in the south with a mean elevation of approximately 2,000 m and the vegetation is luxuriant in the wettest region of Ningxia. It exhibits a typical continental climate with an annual temperature of 5°C–9°C, annual precipitation of 292 mm, and annual evaporation greater than 2,000 mm (Du and Tian, 2012). Climate and vegetation vary in different parts of Ningxia (Chen et al., 2007).

### 2.2 Data sources

The NDVI data set derived from the MODIS sensor has shown excellent performance in monitoring vegetation change and vegetation productivity index. Therefore, it is commonly used in regional vegetation activity monitoring. Data are from the Land Processes Distributed Active Archive Center (LPDAAC). The temporal and spatial resolutions of the data are 16 d and 250 m, respectively. The original NDVI data must be pre-processed by data format conversion, projection transformation, tailoring of the data, etc. Then, the NDVI data are smoothed using the Savitzky-Golay (S-G) method and no-vegetation factors such as aerosol, ice, snow, and sensor observation view angle, which has an impact on the NDVI value, are eliminated to accurately reflect the seasonal change of vegetation (Chen et al., 2004). The maximum NDVI (NDVImax) represents the optimal growth status of vegetation and is used to express the longitudinal variation of vegetation. NDVImax is calculated using the Maximum Value Composite (MVC) method. Our study divided the vegetation growing season into spring (April, May), summer (June, July, August), and autumn (September, October); the monthly average composite NDVI of each season was used to calculate the NDVI of each season (Du et al., 2015).

To examine the corresponding NDVI data time period, continuously observed climatic data sets including the accumulated temperature, accumulated precipitation, sunshine duration, and monthly mean wind velocity data were collected. These meteorological data from 20 meteorological stations were chosen to analyze the trends of climate from 2001 to 2016 in Ningxia. Selected meteorological stations were located in small cities with slight heat island effects. The meteorological stations in this study included those in Huinong, Yinchuan, Taole, Zhongwei, Zhongning, Yanchi, Dingbian, Haiyuan, Tongxin, Guyuan, Xiji, Alashan, Huining, Xifeng, Huanxian, Etuokeqi, Huajialing, Changwu, Jingyuan, and Pingliang (Fig. 1(a)). The monthly accumulated temperature, accumulated precipitation, sunshine duration, and wind velocity data were

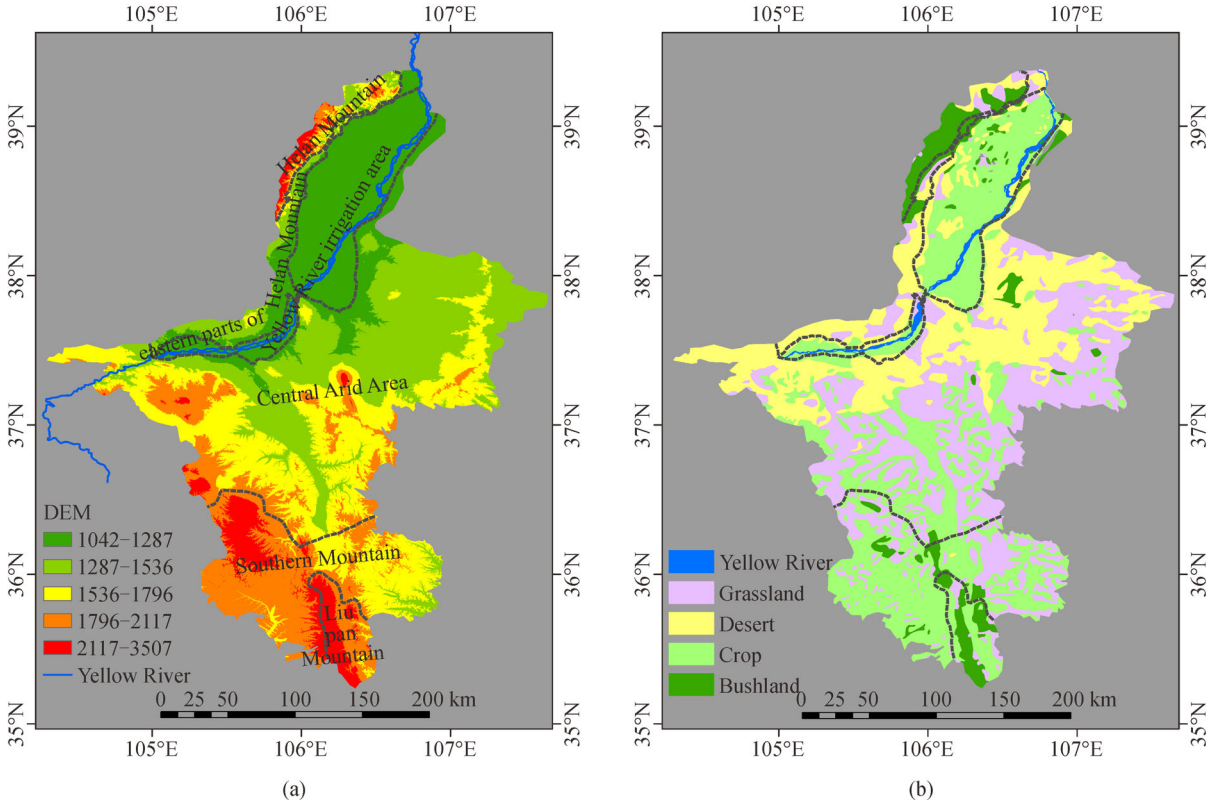


**Fig. 1** Location information (a) and vegetation types (b) of the studied region.

transformed into raster layers with a spatial resolution of 250 m by using the thin plate smooth spline interpolation method (Hutchinson, 1995).

In this study, DEM data were purchased from the International Scientific Data Service Platform. The data of vegetation type was digitized from the 1:1000000 vegetation maps covering Ningxia. To match the resolution of the MODIS NDVI data (250 m), all data were re-sampled with the use of the ArcGIS Resample tool. In addition, the vegetation was classified into four types: bushland, cropland, desert, and grassland. Vegetation category distribution is showed in Fig. 1(b).

## 2.3 Methods

The MODIS Reprojection Tool (MRT) and ArcGIS10.2 were used for data processing. This study calculated the monthly maximum NDVI, accumulated temperature, accumulated precipitation, sunshine duration, and monthly mean wind velocity during 2001–2016. Methods used in this study are as followed:

### 2.3.1 Regression trend line method

During the whole research period, the NDVI trends of each season were detected by using a least-squares simple linear regression model, which can provide the change rate and the significance. It has been widely used in linear time trend calculation (Running and Nemani, 1988).

$$Y = \beta_0 + \beta_1 X + \varepsilon, \tag{1}$$

$Y$ is the NDVI, $X$ is the year, and $\varepsilon$ is the residual error.

Regression trend line algorithm is a regression method that is applied in analysis of intime series (Song and Ma, 2008). To investigate the change trends of NDVI, a regression trend line algorithm is used to get the change trend of vegetation NDVI during 2001–2016 by calculating per-pixel vegetation NDVI. Its expression is:

$$\theta_{\text{slope}} = \frac{n \times \Sigma_{k=1}^{n}(k \times \text{NDVI}_k) - (\Sigma_{k=1}^{n} k)(\Sigma_{k=1}^{n} \text{NDVI}_k)}{n \times \Sigma_{k=1}^{n} k^2 - (\Sigma_{k=1}^{n} k)^2}, \tag{2}$$

where $n$ represents the year ($n$ = 16); $k$ represents the time series ($k$ = 2001, 2002, …, 2016); $\text{NDVI}_k$ represents NDVImax of the $k^{\text{th}}$ year. $\theta_{\text{slope}}$ is the change rate of NDVI variation; $F$ test was used to test the significance. Based on slope and significance values, the study is divided into the following four grades: insignificant decrease ($\theta_{\text{slope}} < 0$ and $p > 0.05$), significant decrease ($\theta_{\text{slope}} < 0$ and $p \leqslant 0.05$), insignificant increase ($\theta_{\text{slope}} \geqslant 0$ and $p > 0.05$) and significant increase ($\theta_{\text{slope}} \geqslant 0$ and $p \leqslant 0.05$). The total percentage of NDVI change (TPC) refers to the ratio of slope to initial value following Ma and Veroustraete

(2006):

$$\mathrm{TPC} = \frac{(n-1) \times \theta_{\mathrm{slope}}}{\frac{1}{n}\Sigma_{i=1}^{n}\mathrm{NDVI}_i} \times 100. \quad (3)$$

2.3.2 Hurst exponent

The Hurst exponent ($H$) was employed to quantitatively describe the sustainability of the long time series. It is largely applied to climatology, economics, and other fields (Guli Jiapaer et al. 2015). Currently, $H$ is commonly used in climatology and vegetation to assess the persistence of long-term change (Jiang et al. 2017). The expression of $H$ is:

The mean time sequence $\overline{\mathrm{NDVI}}_{(\tau)}$:

$$\overline{\mathrm{NDVI}}_{(\tau)} = \frac{1}{\tau}\Sigma_{t=1}^{\tau}\mathrm{NDVI}_{(\tau)}. \quad (4)$$

The cumulative deviation sequence $X_{(m,\tau)}$:

$$X_{(m,\tau)} = \Sigma_{t=1}^{m}\left(\mathrm{NDVI}_{(t)} - \overline{\mathrm{NDVI}}_{(\tau)}\right),\ 1 \leqslant m \leqslant \tau. \quad (5)$$

The range sequence $R_{(\tau)}$:

$$R_{(\tau)} = \max_{1 \ll m \ll \tau} X_{(m,\tau)} - \min_{1 \ll m \ll \tau} X_{(m,\tau)}. \quad (6)$$

The standard deviation sequence $S_{(\tau)}$:

$$S_{(\tau)} = \left[\frac{1}{\tau}\Sigma_{t}^{\tau}\left(\mathrm{NDVI}_{(t)} - \mathrm{NDVI}_{\tau}\right)^2\right]^{\frac{1}{2}}. \quad (7)$$

The Hurst exponent:

$$\frac{R_{(\tau)}}{S_{(\tau)}} = (\mathrm{c}\tau)^{H}, \quad (8)$$

where: c represents a constant. Both sides of Eq. (8) are picked up the logarithm to get the Hurst experimental formula. A cluster of $H$ values was calculated by least square fitting. The slope of the resulting line was the corrected $H$, which revealed the fractal features of the long series.

$H$ comes in three forms: when $H = 0.5$, the series are random without temporal correlation. When $0 < H < 0.5$, changes in the future are not in line with the changes in the past, i.e., the process is not sustainable. When $H > 0.5$, future changes are in line with past changes, and the process is sustainable. The greater $H$ is, the more sustainable it is. According to the change of $H$ index, the following four levels are defined: strong anti-sustainability ($0 < H \leqslant 0.35$), weak anti-sustainability ($0.35 < H < 0.5$), weak sustainability ($0.5 < H \leqslant 0.65$), and strong sustainability ($0.65 < H \leqslant 1$).

2.3.3 Correlation between NDVI and climate factors

The method (Lu et al., 2006) of "linear fitting + residual analysis" is adopted to do spatial interpolations of accumulated temperature, accumulated precipitation, sunshine duration, and mean wind velocity. The spatiotemporal change of the climate change trends in the studied area is analyzed by spatial analysis functions. Relations between NDVI and climatic factors are analyzed using the analysis method of multiple correlations. The multiple correlation can be obtained by Eq. (9) (Zhang et al., 2013a).

$$r_{xy} = \frac{\Sigma_{i=1}^{n}(x_i - \overline{x})(y_i - \overline{y})}{\sqrt{\Sigma_{i=1}^{n}(x_i - \overline{x})^2 (y_i - \overline{y})^2}}, \quad (9)$$

where $x_i$ and $y_i$ are $x$ and $y$ values in $i^{\mathrm{th}}$ year, respectively; $\overline{x}$ and $\overline{y}$ are indicative of mean value of $x$ and $y$, and $n$ is number of the total of samples. Significant value of NDVI and climate factors scores were found through $t$-test. According to the results, the correlation was divided into four grades: significant positive correlation ($r \geqslant 0$ and $p \leqslant 0.05$), insignificant positive correlation ($r \geqslant 0$ and $p > 0.05$), significant negative correlation ($r < 0$ and $p \leqslant 0.05$), and insignificant negative correlation ($r < 0$ and $p > 0.05$).

## 3 Results

### 3.1 Change of NDVI and its relation with climate

Change in NDVI and climate parameters was calculated (Table 1). The growing season NDVI (GSN) of vegetation maintained a growth trend with the growth rate of $0.42 \times 10^{-2}$/yr from 2001 to 2016 across Ningxia. Accumulated precipitation had increased by 0.87 mm/yr, but did not change significantly. The GSN was positively related to precipitation ($r = 0.48$ and $p < 0.01$). The NDVI during different seasons varied. Spring NDVI (SRN) had increased by $0.22 \times 10^{-2}$/yr from 2001 to 2016. The change in SRN was not in conformity with temperature and precipitation. The trends increased dramatically in the summer NDVI (SMN) and autumn NDVI (ATN) from 2001 to 2016. The change tendencies of SMN and summer precipitation were not consistent during the time period, possibly because of a lag behind precipitation, indicating a "time lag effect" (Gu et al., 2018). In autumn, change in ATN and climate parameters was not significantly correlated. Wind velocity had a significant negative effect on the NDVI in autumn ($r = -0.65$ and $p < 0.01$), followed by summer ($r = -0.62$ and $p < 0.01$), growing season ($r = -0.56$ and $p < 0.01$), and spring ($r = -0.39$). In addition, sunshine duration had no significant correlation with NDVI.

**Table 1** Change trends of NDVI and climate parameters during 2001–2016. The ratios are proved by a simple linear regression model ($R^2$ value)

| Time period | NDVI ($\times 10^{-2}$/yr) | Temperature (°C/yr) | Precipitation (mm/yr) | Sunshine duration (h/yr) | Wind velocity (m/(s·yr$^{-1}$)) |
|---|---|---|---|---|---|
| GSN | 0.42** | 0.17 | 0.87 | 1.13 | −0.05** |
| | (0.56) | (0.31) | (0.09) | (0.13) | (0.63) |
| SRN | 0.22* | 0.08 | 1.07 | 1.81 | −0.06** |
| | (0.36) | (0.26) | (0.26) | (0.10) | (0.72) |
| SMN | 0.55** | 0.03 | −1.11 | 0.90 | −0.04** |
| | (0.43) | (0.06) | (0.05) | (0.02) | (0.56) |
| ATN | 0.48** | 0.07 | 1.81 | 0.86 | −0.04** |
| | (0.34) | (0.07) | (0.05) | (0.01) | (0.48) |

** and * stand for $p < 0.01$ and $p < 0.05$, respectively

### 3.2 Spatial variation pattern of NDVI and sustainability of vegetation variation

Spatial distribution of NDVI is presented in Fig. 2. Spatial heterogenous patterns in the GSN trend from 2001 to 2016 were observed (Fig. 2(a)) in which the GSN had a tendency to increase (Table 2). GSN increased in most vegetated areas (88.7%), particularly in the eastern Helan Mountains, the central arid area, the southern mountains, and the Liupan Mountains. A small fraction of vegetated areas (2.7%) showed a significantly increased GSN, particularly in the central arid area and southern mountains. Areas with significant decreasing trend in GSN were infrequent (0.7%), including the Helan Mountains and Yellow River irrigation areas. NDVI with a significant increase occurred in fewer areas in the spring than in the growing season from 2001 to 2016. Most areas (83%) with increases in SRN were located in the central arid area, southern mountains, and the Liupan Mountains. Few areas (2.0%) with significant increase in SRN included the central arid area, southern mountains, and the Liupan Mountains (Fig. 2(b)). Significant decrease in SRN was primarily found in the Yellow River irrigation area (4.7%) with cultivated land and concentrated human activity (Chen et al., 2007). Cultivated land had decreased in this region during 2000–2015 (Cadavid Restrepo et al., 2017). The spatial patterns of the SMN trend were different from that of the GSN and SRN trends from 2001 to 2016, and areas with significant increase in SMN (24.9%) were situated in the southern mountain (Fig. 2(c)), where cultivated land increased and crops flourished in summer (Cadavid Restrepo et al., 2017). The spatial variation pattern of ATN was similar to GSN from 2001 to 2016 (Fig. 2(d)). The area percentage with a significant increase in ATN was 5.8%, and the area percentage with a significant decrease in ATN was 0.8%.

Using the Hurst exponent, the complexity of vegetation change trend and the prediction of the future change trend was examined, and the $H$ spatial pattern of NDVI from 2001 to 2016 was calculated (Figs. 3 and 4). Depending on the $H$, a positive sustainability sequence occupies most vegetation coverage areas in each season. In addition, from 2001 to 2016, vegetation degradation areas of Ningxia accounted for 11.3%, 17%, 13.7%, and 11.1% of the total vegetated areas in the growing season and each season. Thus, the vegetation in most areas of Ningxia continues to expand. The anti-sustainability sequence is primarily distributed in the central arid area, which is distant from the river and maintains poor soil moisture conditions. Besides, increasing temperature accelerates local drought and causes vegetation degeneration. The proportion of anti-sustainability sequences was 12.42% and that of sustainability sequences was 87.58% in the growing season. The proportion of strong anti-sustainability sequences, weak anti-sustainability sequences, weak sustainability sequences, and strong sustainability sequences was 0.32%, 12.1%, 46.29%, and 41.29%, respectively (Fig. 4(a)). In each season, the proportion of anti-sustainability sequences were 21.38%, 20.41%, and 14.87%, respectively, and that of sustainability sequences were 78.62%, 79.59%, and 85.13%, respectively (Fig. 4(a)–(c)). The mean value of the Hurst exponent in the entire region was 0.55 in the growing season, summer season, and the autumn season, whereas it was 0.54 in spring. Most areas presented $H$ greater than 0.5, indicating weak sustainability. $H$ between 0.5 and 0.65 was frequently observed, indicating that the vegetation cover change in Ningxia will have explicit sustainability in the future.

**Table 2** The percentages of variation types in the vegetated NDVI

| Variation types | GSN | SRN | SMN | ATN |
|---|---|---|---|---|
| Insignificant decrease | 10.6 | 12.3 | 12.0 | 10.3 |
| Significant decrease | 0.7 | 4.7 | 1.7 | 0.8 |
| Insignificant increase | 86.0 | 81.0 | 61.4 | 83.1 |
| Significant increase | 2.7 | 2.0 | 24.9 | 5.8 |

### 3.3 The correlation between NDVI and climate parameters

Relations of spatial patterns were analyzed from 2001 to 2016 to discuss the influence of regional climate variation

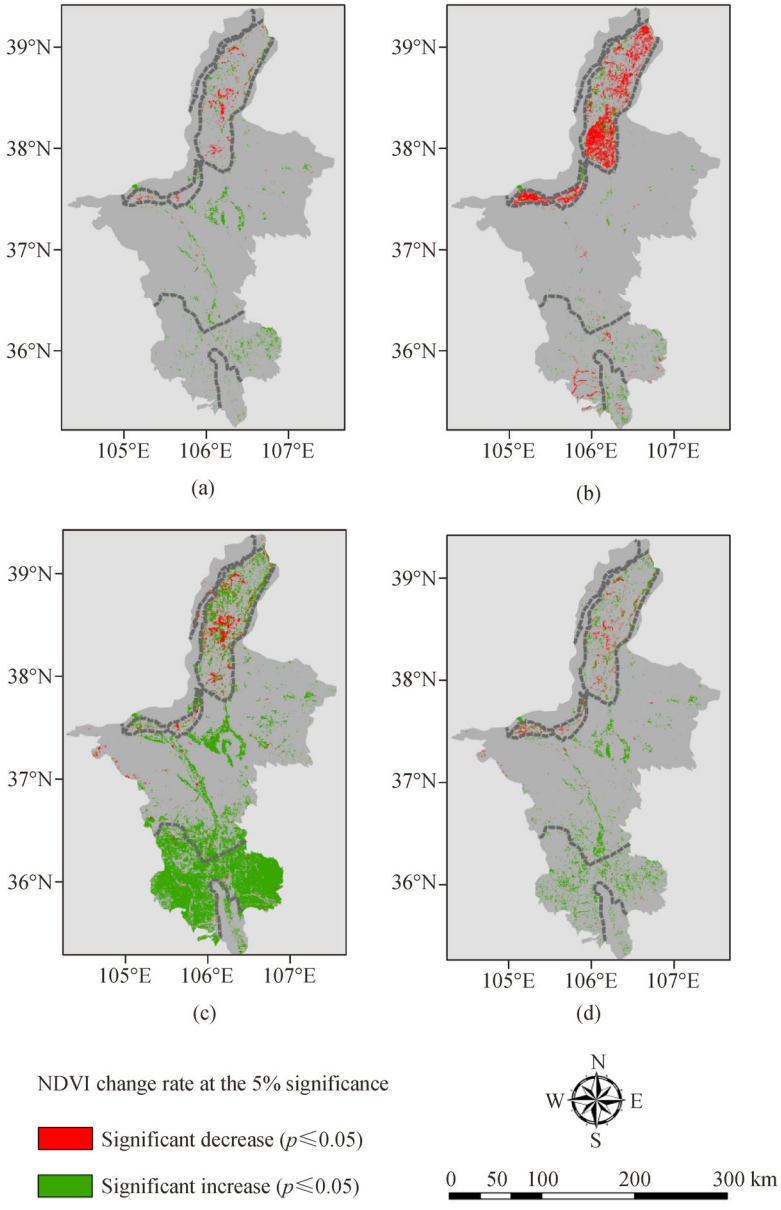


**Fig. 2** Spatial variation pattern of NDVI in seasonality in studied region from 2001 to 2016.

on NDVI in Ningxia (Table 3, Fig. 5). As showed in Fig. 5, correlations among NDVI, the current sunshine duration, temperature, precipitation, and wind velocity were obvious in each season. The NDVI had lower significant correlation with temperature. But the significantly negative correlation of NDVI and temperature occurred in a minority of vegetation areas (7.5%) in the summer. More pixels exhibited a significantly positive correlation between the NDVI and precipitation in spring (30.3%) than that in the growing season (17.8%), autumn (15.1%), and summer (7.2%). These pixels were discovered in the western regions of the central arid area and southern mountains (Figs. 5(b), 5(f), 5(j), 5(n)). However, the NDVI and precipitation showed no significantly negative correlation in the Yellow River irrigated area and the Liupan Mountains, in which precipitation and grassland NDVI increased dramatically while NDVI decreased. The case was usually found in humid regions (Gu et al., 2018). Pixels with a significantly negative correlation between the NDVI and sunshine duration in the growing season (13.2%) opposed to those in summer (12.7%), autumn (10.2%), and spring (9.1%). These pixels were distributed in the central arid area, southern mountains, and Liupan Mountains in Ningxia. The correlation between the NDVI and sunshine duration in the Yellow River irrigation area was decisive in the growing season and summer (Figs. 5

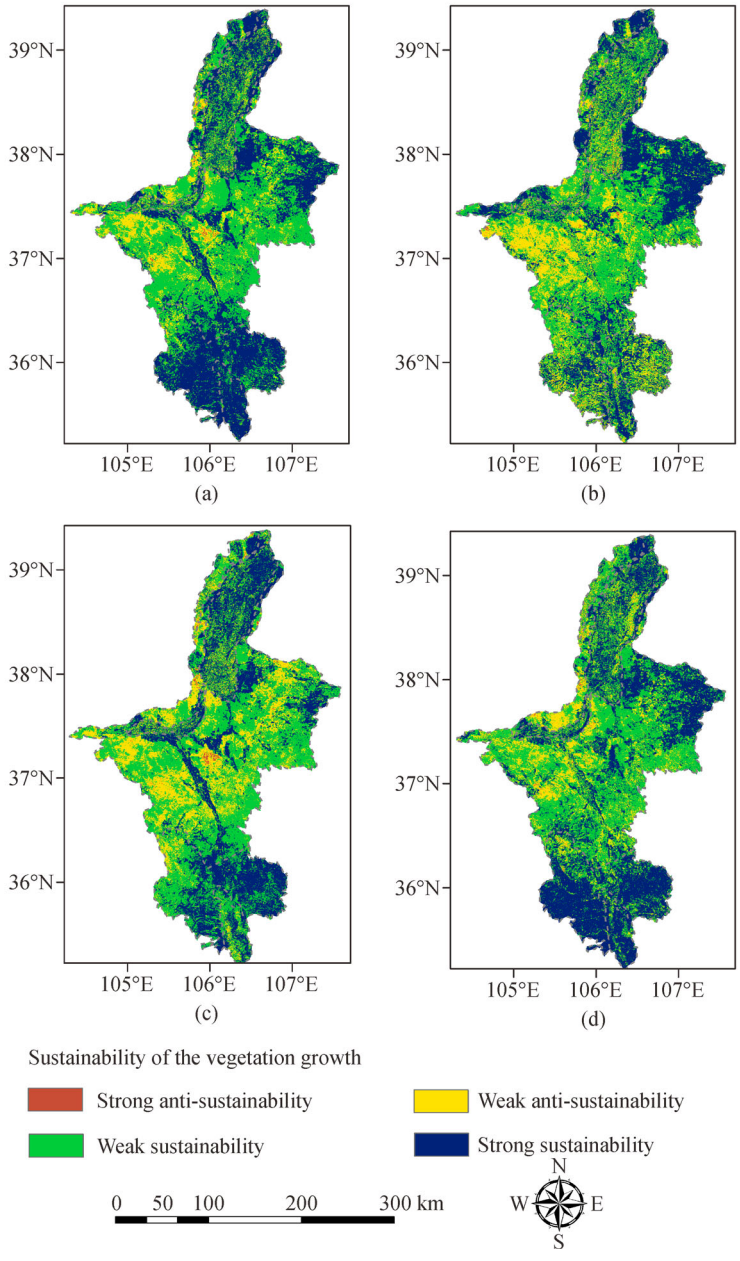


**Fig. 3** *H* spatial pattern of NDVI in studied region from 2001 to 2016.

(c), 5(g), 5(k), 5(o)). More pixels exhibited significantly negative correlation between the NDVI and wind velocity in spring (20.7%) than that in autumn (19.8%) and the growing season (14.3%), especially in the central arid area, Yellow River irrigation area, southern and Liupan Mountains. In summer, the NDVI and wind velocity had a significantly negative correlation in the Yellow River irrigation area (3.2%). The NDVI of the central arid area, southern mountains and Liupan Mountains was positively correlated with wind velocity in summer, accounting for 74.4% of the vegetation areas (10.4% with a significant correlation) (Table 3, Figs. 5(d), 5(h), 5(l), 5(p)).

As showed in Fig. 6, the sensitivity of vegetation to climate change was distinct among different vegetation types. Thus, under different weather conditions, the responses of the same vegetation were variable (Xu et al., 2016). Bushlands responded more strongly to sunshine duration and wind velocity than to temperature and precipitation (Fig. 6). Bushland NDVI was a positive correlation with temperature and precipitation in the growing season, spring season, and the summer season (Figs. 6(a), 6(e), 6(i)), whereas there was no correlation in autumn. Bushland NDVI had a negative correlation with sunshine duration and wind velocity in growing season,

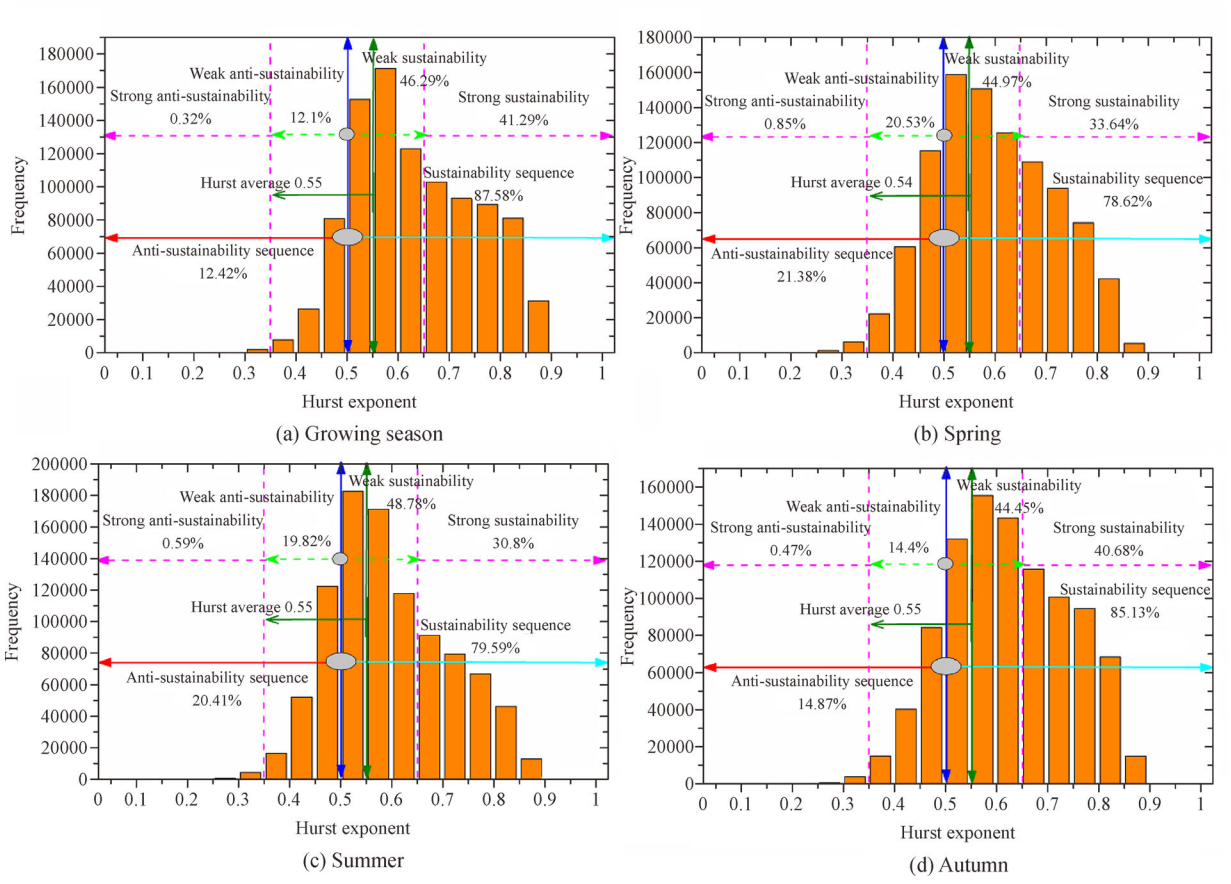


**Fig. 4** Predicted results of NDVI of Ningxia in the future.

**Table 3** Correlation percentages of NDVI and climate parameters in each season

| Time period | Variation types | $R_{NDVI-T}$ | $R_{NDVI-P}$ | $R_{NDVI-S}$ | $R_{NDVI-W}$ |
|---|---|---|---|---|---|
| GSN | Significant positive correlation | 1.4 | 17.8 | 4.5 | 1.1 |
| | Insignificant positive correlation | 43.5 | 56.4 | 29.3 | 21.8 |
| | Significant negative correlation | 0.2 | 0.1 | 13.2 | 14.3 |
| | Insignificant negative correlation | 54.9 | 25.7 | 53.0 | 62.8 |
| SRN | Significant positive correlation | 3.2 | 30.3 | 2.7 | 3.7 |
| | Insignificant positive correlation | 40.8 | 56.4 | 33.3 | 16.5 |
| | Significant negative correlation | 6.6 | 0.6 | 9.1 | 20.7 |
| | Insignificant negative correlation | 49.4 | 12.6 | 54.9 | 59.1 |
| SMN | Significant positive correlation | 0.1 | 7.2 | 3.4 | 10.4 |
| | Insignificant positive correlation | 16.7 | 58.5 | 21.7 | 64.0 |
| | Significant negative correlation | 7.5 | 0.5 | 12.7 | 3.2 |
| | Insignificant negative correlation | 75.7 | 33.8 | 62.2 | 22.4 |
| ATN | Significant positive correlation | 3.2 | 15.1 | 1.0 | 0.3 |
| | Insignificant positive correlation | 37.8 | 71.0 | 25.1 | 8.7 |
| | Significant negative correlation | 3.9 | 0.2 | 10.2 | 19.8 |
| | Insignificant negative correlation | 55.1 | 13.7 | 63.7 | 71.2 |

spring season, and autumn season, whereas there was a positive correlation in summer. Significantly positive correlations between bushland NDVI and precipitation were observed in more pixels in spring (13.63%) than in autumn (4.37%), summer (2.92%), and the growing season (1.75%).

The correlation between GSN and precipitation was significantly positive, and was found in most of the deserts (32.74%), grasslands (26.22%), and croplands (16.40%). These pixels presented a definite correlation between SRN and precipitation, and the ratios of all pixels included 31.45%, 28.89%, and 17.07% for croplands, grasslands, and deserts, respectively. The SRN and temperature showed a positive correlation and were 4.09%, 2.92%, and 1.04% for croplands, deserts, and grasslands, respectively. In autumn season, the NDVI and precipitation exhibited a positive correlation which was 19.43%, 15.09%, and 11.51% for croplands, grasslands, and deserts, respectively. As showed in Fig. 6, under the same climatic factor, the influence of climate variation on vegetation was distinct among various vegetation types. Table 4 showed proportions of a significantly positive correlation between NDVI and temperature, which were observed in bushlands, croplands, deserts, and grasslands in spring. The NDVI and precipitation showed significant positive correlations for deserts and grasslands, which were higher than croplands and bushlands in the growing season and summer season, the same as croplands and grasslands are higher than deserts and bushlands in the spring season and the autumn season. Deserts, grasslands, and croplands NDVI and sunshine duration presented significantly negative correlations in each season. NDVI was significantly negatively correlated with wind velocity in deserts, grasslands, and croplands in growing season, spring season, and autumn season, whereas in summer, there was a significantly positive trend in grasslands (17.34%), deserts (8.15%), and croplands (6.69%).

## 4 Discussion

### 4.1 The effect of climate parameters on NDVI

Climate change strongly impacts vegetation variations (Zhu et al., 2016). This research indicated that climate change deeply impacted the vegetation dynamics in Ningxia (Fig. 5). This result is consistent with other results from central Asia (Mohammat et al., 2013). Positive correlations with GSN and precipitation in the most regions (74.2%) in Ningxia were observed (Table 3), suggesting that precipitation primarily affected the vegetation variation in arid and semi-arid areas (Xu et al., 2017). The reduction of precipitation could lower the soil moisture and accelerate drought, leading to the reduction of photosynthesis (Fensholt and Proud, 2012). We concluded that the GSN and temperature in the Yellow River irrigated area had a significant positive correlation. Kang et al. (2011) showed that rising temperatures promoted vegetation growth in the wetter areas. Zhou et al. (2015) suggested that rising temperatures promoted vegetation growth in most of central Asia but also inhibited growth by increasing evapotranspiration. The main reason for this inconsistency is that the vegetation response to temperature varied in different dry and wet conditions and with vegetation types (Li et al., 2011). GSN and sunshine duration had a significant negative correlation in the central arid area, southern mountains and Liupan Mountains, whereas GSN and sunshine duration in the Yellow River irrigation area had a significant positive correlation. This result is due to the decreased precipitation in the central

**Table 4** Percentages of correlation in different vegetation types during 2001-2016

| Vegetation type | Growing season | | | | | | | | Spring | | | | | | | |
|---|---|---|---|---|---|---|---|---|---|---|---|---|---|---|---|---|
| | $R_{NDVI-T}$ | | $R_{NDVI-P}$ | | $R_{NDVI-S}$ | | $R_{NDVI-W}$ | | $R_{NDVI-T}$ | | $R_{NDVI-P}$ | | $R_{NDVI-S}$ | | $R_{NDVI-W}$ | |
| | SP | SN | SP | SN | SP | SN | SP | SN | SP | SN | SP | SN | SP | SN | SP | SN |
| bushland | 0.31 | 1.07 | 1.75 | 0.01 | 1.94 | 25.23 | 2.18 | 17.51 | 8.59 | 2.42 | 13.63 | 3.07 | 2.67 | 10.42 | 1.21 | 29.51 |
| cropland | 1.17 | 8.25 | 16.40 | 0.18 | 6.24 | 17.01 | 1.75 | 14.08 | 4.09 | 8.90 | 31.45 | 0.97 | 2.13 | 11.49 | 7.94 | 17.34 |
| desert | 0.05 | 8.78 | 32.74 | 0.03 | 5.73 | 5.53 | 0.57 | 21.65 | 2.92 | 4.10 | 17.07 | 0.18 | 5.21 | 3.50 | 1.73 | 26.35 |
| grassland | 0.05 | 12.95 | 26.22 | 0.04 | 1.25 | 12.84 | 0.36 | 6.66 | 1.04 | 5.24 | 28.89 | 0.05 | 0.97 | 10.61 | 0.46 | 18.00 |
| Vegetation type | Summer | | | | | | | | Autumn | | | | | | | |
| | $R_{NDVI-T}$ | | $R_{NDVI-P}$ | | $R_{NDVI-S}$ | | $R_{NDVI-W}$ | | $R_{NDVI-T}$ | | $R_{NDVI-P}$ | | $R_{NDVI-S}$ | | $R_{NDVI-W}$ | |
| | SP | SN | SP | SN | SP | SN | SP | SN | SP | SN | SP | SN | SP | SN | SP | SN |
| bushland | 0.55 | 0.27 | 2.92 | 0.69 | 0.83 | 16.23 | 8.05 | 2.05 | 0.28 | 12.52 | 4.37 | 0.23 | 4.36 | 8.34 | 1.48 | 19.13 |
| cropland | 0.68 | 3.48 | 4.20 | 0.40 | 5.13 | 16.65 | 6.69 | 5.73 | 2.73 | 3.03 | 19.43 | 0.29 | 0.92 | 12.66 | 0.36 | 20.34 |
| desert | 0.27 | 2.37 | 23.02 | 0.09 | 4.45 | 5.82 | 8.15 | 2.60 | 0.41 | 6.63 | 11.51 | 0.14 | 0.79 | 8.94 | 0.15 | 23.15 |
| grassland | 0.03 | 3.95 | 10.40 | 0.02 | 0.67 | 13.51 | 17.34 | 0.33 | 2.38 | 5.60 | 15.09 | 0.05 | 0.33 | 9.33 | 0.06 | 15.74 |

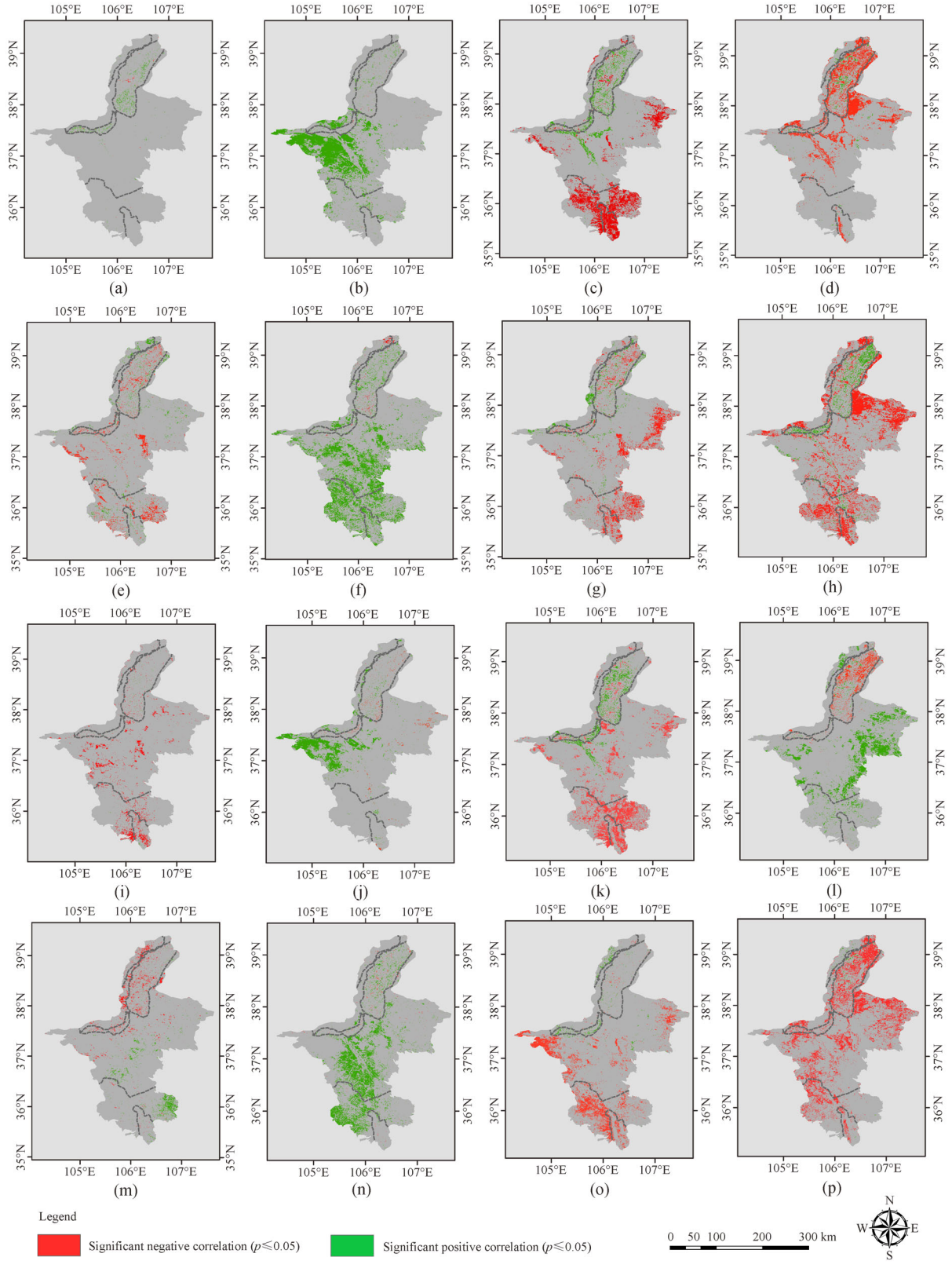


**Fig. 5** Spatial significant correlation distribution with NDVI and climate parameters. (a) GSN and temperature, (b) GSN and precipitation, (c) GSN and sunshine duration, (d) GSN and wind velocity, (e) SRN and temperature, (f) SRN and precipitation, (g) SRN and sunshine duration, (h) SRN and wind velocity, (i) SMN and temperature, (j) SMN and precipitation, (k) SMN and sunshine duration, (l) SMN and wind velocity, (m) ATN and temperature, (n) ATN and precipitation, (o) ATN and sunshine duration, and (p) ATN and wind velocity.

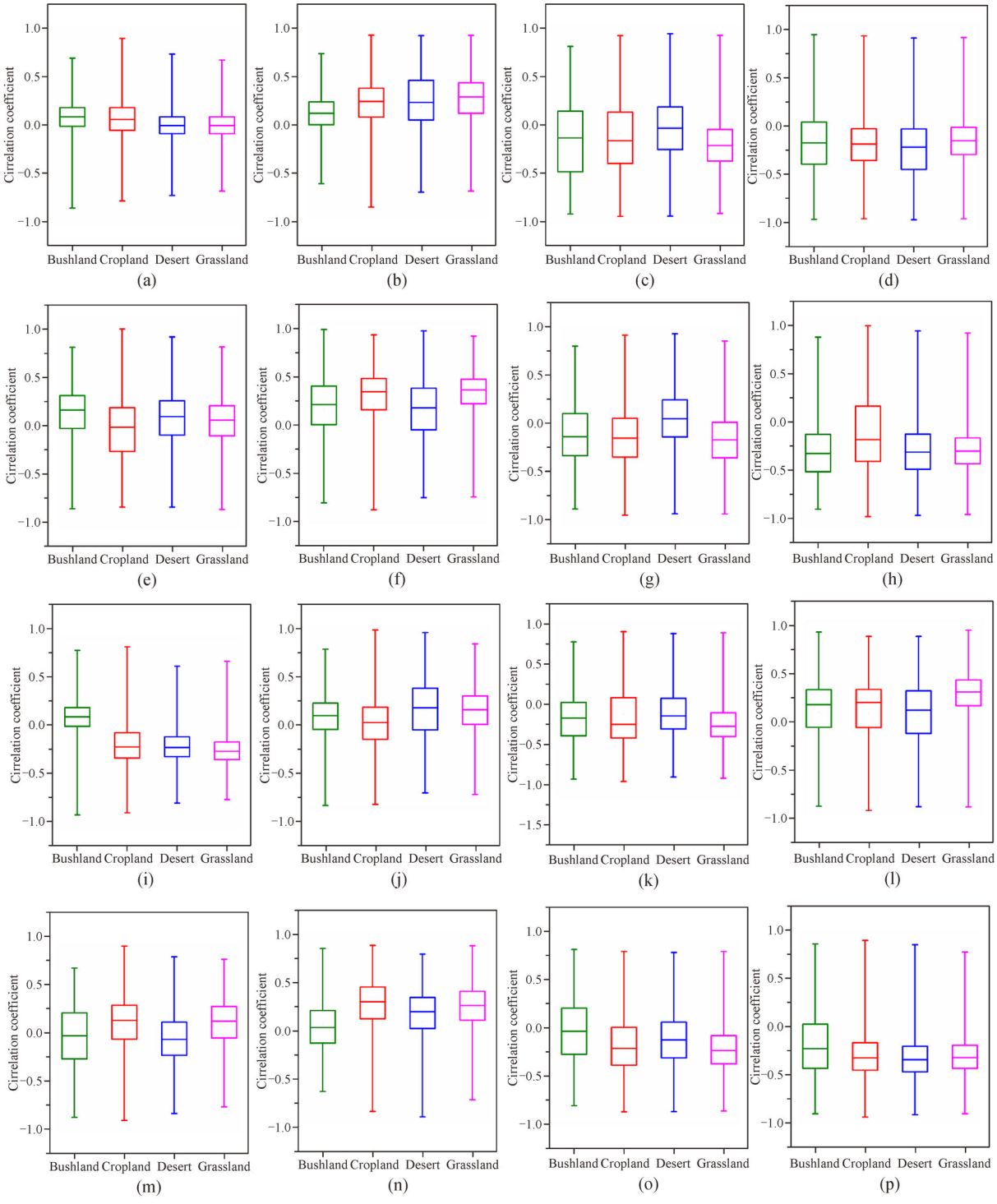


**Fig. 6** Correlation between NDVI and climatic parameters in various vegetated types (a) GSN and temperature, (b) GSN and precipitation, (c) GSN and sunshine duration, (d) GSN and wind velocity, (e) SRN and temperature, (f) SRN and precipitation, (g) SRN and sunshine duration, (h) SRN and wind velocity, (i) SMN and temperature, (j) SMN and precipitation, (k) SMN and sunshine duration, (l) SMN and wind velocity, (m) ATN and temperature, (n) ATN and precipitation, (o) ATN and sunshine duration, and (p) ATN and wind velocity. Box-whisker Plot: the whole quartile spacing box is values of 25th and 75th percentiles; horizontal line represents median; the upper and lower limits of the whisker represent the maximum and minimum values.

arid area, southern mountains, and Liupan Mountains. Reduced precipitation can lower soil water content and increase sunshine duration, which further reduced the soil water content and directly restricted the growth of vegetation (Zhang, 2017). There was extreme precipitation in the Yellow River irrigation area and abundant accumulation of soil water for many years. When temperature and sunshine duration increased, the natural conditions that were needed for the growth and development of vegetation were achieved (Zhang, 2017). We observed a significantly negative correlation between the GSN and wind velocity in most parts of Ningxia, which was in agreement with the results on the Tibetan plateau (Yao, 2018). Wind stress increased the transpiration rate of plants and affected the relative humidity and temperature (Zhang et al., 2013b). Therefore, wind velocity was negatively correlated with vegetation growth.

Among the NDVI, temperature and precipitation showed a higher score in spring and autumn and a lower score in summer (Table 3). This result suggested that the vegetation in Ningxia was susceptible to heat and the temperature and precipitation limited the vegetation growing season. The results showed that increasing temperature and precipitation promoted vegetation growth during the spring. Higher temperatures in spring may speed up the development of organisms in the body, such as in phenology in the spring (Kariyeva and Leeuwen, 2011). Earlier snow melts from rapid warming enhances soil moisture, leading to vegetation growth (Guli·Jiapaer et al., 2015). Additionally, with temperatures increase in the spring, sufficient precipitation mitigates drought stress (Gessner et al., 2013). In spring, precipitation can regulate the response of vegetation to temperature effects on water availability. The SMN exhibited a positive correlation to the precipitation, but negatively correlated with temperature (Fig. 5). This result showed that the effect on vegetation in water-limited ecosystems was negative (Zhao et al., 2015). Xu et al. (2017) found vegetation degradation related to a decrease in precipitation and an increase in temperature in Central Asia. The regional spatial distribution of NDVI and autumn temperatures was comparable to that of spring (Fig. 4), indicating that the trends of NDVI in summer and autumn result from increased drought stress caused by warming and unchanged precipitation. Significant negative correlations with the NDVI and sunshine duration were found in summer (12.7%) compared to autumn (10.2%) and spring (9.1%), which was in line with the growing season. Pixels with a significantly negative correlation between NDVI and wind velocity in spring distributed in the eastern central arid area, Helan Mountains, eastern parts of the Helan Mountains, southern mountains, and Liupan Mountains. The eastern central arid area, Helan Mountains and the eastern, parts of the Helan Mountains located at the leading edge of the Tengger Desert, Mu Us Desert and Ulan Buh Desert, where wind causes erosion and is accompanied by dust events (Jiang and Zhang, 2016). Wind velocity in spring causes frequent sand and salt dust weather events such as soil salt accumulation considerably increases and soil moisture decreases. Thus, only salt-tolerant and drought-tolerant vegetation was present, which affected the vegetation coverage in spring (Sun et al., 2018; Yao, 2018). The NDVI in the central arid area and southern mountains was significantly positively correlated with wind velocity in summer, possibly because the climate was relatively humid and vegetation was largely affected by temperature and precipitation (Yao, 2018). Another possibility is that the vegetation was resistant to wind (Zhang et al., 2013b).

Past studies have demonstrated that the influence of climatic parameters on NDVI has a “time lag effect” (Gu et al., 2018). It is undeniable that NDVI and climatic parameters have significantly spatiotemporal heterogeneity relations. The change of NDVI was comparable to that of climate parameters, but the time point did not correspond to the extreme value time of climate parameters. Variations in NDVI lagged behind climate parameters, showing a “time lag effect.” To compare the time lag effect on climate parameters, the previous season (i.e., winter temperature and SRN) and the current season (i.e., spring temperature and SRN) were used as time intervals. We calculated the correlations of NDVI and climate parameters (Table 5). The response of NDVI to climatic parameters of the preceding and current season was different. Table 5 showed that the SMN and spring precipitation was a significantly positive correlation ($r = 0.51$ and $p < 0.01$). Sufficient precipitation in spring could mitigate drought stress and regulate the response of vegetation to temperature effects on water availability (Gessner et al., 2013). Historical study has also shown that early accumulated precipitation affects seasonal phenotypes in arid and semi-arid regions (Jenerette et al., 2010).

Vegetation growth in Ningxia reflected by the NDVI increased from 2001 to 2016. However, our research suggested that the change of NDVI was likely affected by climate parameters in the restricted water ecosystem. The weather data showed that the mean temperature was 9.17°C from 2001 to 2016 in Ningxia. Thermal conditions restricted the growth of vegetation. Rising temperatures resulted in early growth and increase of vegetation growth. The increase of temperature could influence the evaporation and transpiration of vegetation (Zhao et al., 2011). However, these results are distinct with the global model, and past studies have demonstrated that the NDVI has a positive correlation to warmer temperatures in the Northern Hemisphere (Zhao et al., 2011). In addition, under many conditions, the relations between NDVI and climate were not strong, suggesting that there are numerous uncertainties in this field. The most likely reason was human activity, especially the Grain for Green Project (GGP). Compared to decrease vegetation, the increased vegetation showed much more change (Table 2). The

**Table 5** Relations between NDVI and climate parameters from 2001 to 2016

| Time period | Temperature | | Precipitation | | Sunshine duration | | Wind velocity | |
|---|---|---|---|---|---|---|---|---|
| | previous season | same season | previous season | same season | previous season | same season | previous season | same season |
| SRN | 0.293 | 0.117 | 0.234 | 0.636** | −0.043 | −0.059 | −0.385 | −0.436 |
| SMN | 0.014 | −0.136 | 0.510** | 0.286 | 0.122 | −0.107 | −0.562* | −0.573* |
| ATN | −0.297 | −0.106 | 0.166 | 0.302 | −0.272 | −0.103 | −0.688** | −0.637** |

** and * stand for $p < 0.01$ and $p < 0.05$, respectively

vegetation in most areas had an increasing trend, which was in line with the study results in south-west of China (Cheng et al., 2017; Gu et al., 2018). The GGP decreased cropland and increased forests and grasslands. Cadavid Restrepo et al. (2017) assessed and quantified the spatiotemporal dynamics of land cover in Ningxia, and the results showed that the land cover change reflected the goal of the national policy on restoration of degraded land during 2000–2015. Due to the conversion of herbaceous vegetation (53.8%) and cropland (30.8%), the increasing forestland was of significant change of land use over the study period.

### 4.2 The effect of climate parameters on different vegetation types

The impact of climate change on vegetation was distinct among different vegetation types (Xu et al., 2018). This study showed that each vegetation type was more sensitive to precipitation than to temperature (Fig. 6), which may be caused by extreme sensitivity to inter-annual precipitation variability. With smaller root systems, vegetation has a limited ability to maintain soil moisture (Propastin, 2008). Vegetation growth needed precipitation (63.8%) in the arid area of north China (Xu and Wang, 2016). Nearly 80% of surface precipitation in Central Asia was responsive to vegetation change (Gessner et al., 2013). This article indicated the different vegetation had a different response to climate drivers. The positive correlation of grassland NDVI-precipitation was due to the moisture that the vegetation required to grow. Precipitation is useful to vegetation growth in arid areas. In bushland areas (the Liupan Mountains and Yellow River irrigated area), where precipitation is abundant, the negative correlation of NDVI-precipitation is likely to be accompanied by an increase in cloud content due to the increase in precipitation. Table 4 showed that the NDVI and precipitation for each vegetation type were positive. Because the vegetation coverage depends on water for agricultural activities during the rainy period, increased precipitation may induce vegetation growth. On the contrary, the correlation among the NDVI, sunshine duration, and wind velocity for the different vegetation types were negative. In general, sunshine positively affects the growth of vegetation. However, NDVI and sunshine duration in Ningxia showed a slightly negative correlation. The probable reason is that the increase of sunshine leads to the increase of evaporation transpiration. Wind velocity and NDVI had a negative correlation in Ningxia, indicating that the direct effect of wind velocity on evaporation transpiration rates affects the loss of vegetation and soil moisture. The increase of wind velocity and evapotranspiration rate decreases the soil moisture (Sun et al., 2018). Temperature was found to be weakly correlated with each vegetation type, with weak positive correlations among bushland, cropland, and grassland. Rising temperature could increase evaporation and reduce the growth of plants in arid regions (Zhao et al., 2011). Our results increase understanding of vegetation on regional response to climate variation.

## 5 Conclusions

This research demonstrates that climate variation and human activity impacted the spatiotemporal dynamics of NDVI in Ningxia from 2001 to 2016. The vegetation growth reflected by the NDVI increased in each season. Additionally, the trend in NDVI showed the greatest increase in summer and the least increase in spring. Significant increases in vegetation areas occurred in the southern mountains, Liupan Mountains, and central arid areas. The degraded vegetation coverage was located in the Yellow River irrigation area with cultivated land and intense human activity. Most vegetation areas in the southern mountains increased significantly in the summer, being accountable for 24.9% of the total amount. Positive sustainability was predicted in most vegetation coverage areas in Ningxia. Additionally, vegetation in most areas will continue to expand. NDVI showed a positive correlation with precipitation but a weaker correlation with temperature. Sunshine duration and wind velocity had a profound influence on NDVI in Ningxia. The SMN response to precipitation variation demonstrated a time lag effect. The impact of climate change on vegetation was distinct among different vegetation types. A significant role was discovered using the GGP for improving vegetation in Ningxia.

**Acknowledgements** This work is funded by the National Key R&D Program of China (No. 2017YFB0504201), Tianyou Youth Talent Lift Program of Lanzhou Jiaotong University, the Natural Science Foundation of

Gansu Province (No. 17JR5RA095), the Youth Fund of Lanzhou Jiaotong University (No. 2017002), the National Natural Scientific Foundation of China (Grants Nos. 41761014, 41371435, 41761088, 41761082 and 41861059) and LZJTU EP 201806. Thanks for the LPDAAC for providing the MODIS product

## References

Cadavid Restrepo A M, Yang Y R, Hamm N A S, Gray D J, Barnes T S, Williams G M, Soares Magalhães R J, McManus D P, Guo D, Clements A C A (2017). Land cover change during a period of extensive landscape restoration in Ningxia Hui Autonomous Region, China. Sci Total Environ, 598: 669–679

Chen J, Jönsson P, Tamura M, Gu Z, Matsushita B, Eklundh L (2004). A simple method for reconstructing a high-quality NDVI time-series data set based on the Savitzky-Golay filter. Remote Sens Environ, 91(3–4): 332–344

Chen X G, Li J P, Han Y J, Li Z J, Chen B D (2007). Vegetation coverage and its relationships with temperature and precipitation in Ningxia in 1981–2004. Chinese J Ecol, 26(9): 1375–1383

Cheng F Y, Liu S L, Yin Y J, Lu Y H, An N N, Liu X M (2017). The dynamics and main driving factors of coastal vegetation in Guangxi based on MODIS NDVI. Acta Ecol Sin, 37(3): 788–797

Du J, Shu J, Yin J, Yuan X J, Ahati J H, Xiong S S, He P, Liu W L (2015). Analysis on spatio-temporal trends and drivers in vegetation growth during recent decades in Xinjiang, China. Int J Appl Earth Obs, 38(7): 216–228

Du L T, Tian Q J (2011). Spatiotemporal variations of NDVI in Ningxia Hui Autonomous Region. Bull Soil Water Conserv, 31: 208–214 (in Chinese)

Du L T, Tian Q J (2012). Vegetation coverage variation in Ningxia during 1999–2009 and its relationships with climatic factors. J Desert Res, 32: 1479–1485 (in Chinese)

Fensholt R, Proud S R (2012). Evaluation of Earth Observation based global long-term vegetation trends-Comparing GIMMS and MODIS global NDVI time series. Remote Sens Environ, 119(3): 131–147

Gerten D, Schaphoff S, Haberlandt U, Luchta W, Sitch S (2004). Terrestrial vegetation and water balance—hydrological evaluation of a dynamic global vegetation model. J Hydrol (Amst), 286(1–4): 249–270

Gessner U, Naeimi V, Klein I, Kuenzer C, Klein D, Dech S (2013). The relationship between precipitation anomalies and satellite-derived vegetation activity in Central Asia. Global Planet Change, 110(2): 74–87

Ghosh K G (2018). Analysis of rainfall trends and its spatial patterns during the last century over the Gangetic West Bengal, Eastern India. J Geovis Spat Anal, 2(2): 1–18

Gu Z J, Duan X W, Shi Y D, Li Y, Pan X (2018). Spatiotemporal variation in vegetation coverage and its response to climatic factors in the Red River Basin, China. Ecol Indic, 93: 54–64

Guli·Jiapaer S, Liang Q, Yi J, Liu (2015). Vegetation dynamics and responses to recent climate change in Xinjiang using leaf area index as an indicator. Ecol Indic, 58: 64–76

Guo W, Ni X N, Jing D Y, Li S (2014). Spatial-temporal patterns of vegetation dynamics and their relationships to climate variations in Qinghai Lake Basin using MODIS time-series data. J Geogr Sci, 24(6): 1009–1021

Hua T, Wang X M, Zhang C X, Lang L L, Li H (2017). Responses of vegetation activity to drought in northern China. Land Degrad Dev, 28(7): 1913–1921

Hutchinson M F (1995). Interpolating mean rainfall using thin plate smoothing splines. Int J Geogr Inf Sci, 9(4): 385–403

Hu M Q, Mao F, Sun H, Hou Y Y (2011). Study of normalized difference vegetation index variation and its correlation with climate factors in the three-river-source region. Int J Appl Earth Obs, 13(1): 24–33

Jamali S, Seaquist J, Eklundh L, Ardö J (2014). Automated mapping of vegetation trends with polynomials using NDVI imagery over the Sahel. Remote Sens Environ, 141: 79–89

Jenerette G D, Scott R L, Huete A R (2010). Functional differences between summer and winter season rain assessed with MODIS-derived phenology in a semi-arid region. J Veg Sci, 21(1): 16–30

Jiang L, Jiapaer G, Bao A, Guo H, Ndayisaba F (2017). Vegetation dynamics and responses to climate change and human activities in Central Asia. Sci Total Environ, 599: 967–980

Jiang C, Zhang L (2016). Ecosystem change assessment in the Three-river Headwater Region, China: patterns, causes, and implications. Ecol Eng, 93: 24–36

Jin X M, Yu Q S, Xue Z Q (2007). Study on ecological vegetation changes in Ningxia Hui Autonomous Region. Sci Tech Review, 25: 19–22

Kang Y, Li Z C, Tian H, Liu R, Shi X K, Zhang J H (2011). Trend of vegetation evaluation and its responses to climate change over the source region of the Yellow River, Clim. Environ Res, 16(4): 505–512

Kariyeva J, Van Leeuwen W(2011). Environmental drivers of NDVI-based vegetation phenology in central asia. Remote Sens, 3(2): 203–246

Lei H, Yang D, Huang M (2014). Impacts of climate change and vegetation dynamics on runoff in the mountainous region of the Haihe River Basin in the past five decades. J Hydrol (Amst), 511: 786–799

Li H X, Liu G H, Fu B J (2011). Response of vegetation to climate change and human activity based on NDVI in the Three-River Headwaters region. Acta Ecol Sin, 31(19): 5495–5504

Lu Z Y, Yang T B, Guo W Q (2006). Application of the spatial interpolation of rainfall–a case study of the headstream region of the Yellow River. J Lanzhou U. Nat Sci, 42: 11–14

Mao D H, Ling L, Wang Z M, Zhang C H, Ren C Y (2015). Variations in net primary productivity and its relationships with warming climate in the permafrost zone of the Tibetan Plateau. J Geogr Sci, 25(8): 967–977

Mao D, Wang Z, Luo L, Ren C Y (2012). Integrating AVHRR and MODIS data to monitor NDVI changes and their relationships with climatic parameters in Northeast China. Int J Appl Earth Obs, 18: 528–536

Ma M, Frank V (2006). Interannual variability of vegetation cover in the Chinese Heihe River Basin and its relation to meteorological parameters. Int J Remote Sens, 27(16): 3473–3486

Nair H C, Padmalal D, Joseph A, Vinod P G (2017). Delineation of groundwater potential zones in river basins using geospatial tools–an example from southern western Ghats, Kerala, India. J Geovis Spat Anal, 1(1–2): 1–5

Nemani R R (2003). Climate-driven increases in global terrestrial net primary production from 1982 to 1999. Science, 300(5625): 1560–1563

Mohammat A, Wang X H, Xu X T, Peng L P, Yang Y, Zhang X P, Myneni R B, Piao S L (2013). Drought and spring cooling induced recent decrease in vegetation growth in Inner Asia. Agric Meteorol, 178–179: 21–30

Propastin P A (2008). Inter-annual changes in vegetation activities and their relationship to temperature and precipitation in central Asia from 1982 to 2003. J Environ Inform, 12(2): 75–87

Running S W, Nemani R R (1988). Relating seasonal patterns of the AVHRR vegetation index to simulated photosynthesis and transpiration of forests in different climates. Remote Sens Environ, 24(2): 347–367

Song Y, Ma M G (2008). Variation of AVHRR NDVI and its relationship with climate in Chinese Arid and Cold Regions. J Remote Sensing, 12(3): 499–505

Sun Q, Zhang M, Zeng Y B (2018). Effect of precipitation and wind speed on NDVI in Aibi Lake. Southwest China Journal of Agriculture Sciences, 31(11): 2407–2412 (in Chinese)

Wang H L, Chen A, Wang Q F, He B (2015). Drought dynamics and impacts on vegetation in China from 1982 to 2011. Ecol Eng, 75: 303–307

Xu H J, Wang X P, Yang T B (2017). Trend shifts in satellite-derived vegetation growth in Central Eurasia, 1982–2013. Sci Total Environ, 579: 1658–1674

Xu H J, Wang X P (2016). Effects of altered precipitation regimes on plant productivity in the arid region of northern China. Ecol Inform, 31: 137–146

Xu H J, Wang X P, Zhao C Y, Yang X M (2018). Diverse responses of vegetation growth to meteorological drought across climate zones and land biomes in northern China from 1981 to 2014. Agric Meteorol, 262: 1–13

Yao H R (2018). Characteristics of wind speed and atmospheric kinetic energy over the Tibetan Plateau in spring and their relationship with vegetation coverage. Dissertation for the Doctoral Degree. Nanjing: Nanjing University of Information Science & Technology.

Zhang L, Guo H D, Ji L, Lei L P (2013a). Vegetation greenness trend (2000 to 2009) and the climate controls in the Qinghai-Tibetan Plateau. J. Appl. Remote Sens, 7(1): 073572

Zhang L L (2017). Dynamic evolution of vegetation and its climatic driving factors in Liaoning province. Dissertation for the Master's Degree. Dalian: Liaoning Normal University

Zhang L L, Zhao X Y, Yuan H (2013b). Advances in the effects of wind on Plants. ADV EARTHSCI, 28(12): 1349–1353

Zhang T, Wang H (2015). Trend patterns of vegetative coverage and their underlying causes in the deserts of northwest China over 1982–2008. Plos One, 10(5): 10e0126044

Zhao X, Hu H F, Shen H H, Zhou D J, Zhou L M, Myneni R B, Fang J (2015). Satellite-indicated long-term vegetation changes and their drivers on the Mongolian Plateau. Landsc Ecol, 30(9): 1599–1611

Zhao X, Tan K, Zhao S, Fang S (2011). Changing climate affects vegetation growth in the arid region of the northwestern China. J Arid Environ, 75(10): 946–952

Zhu Z, Piao S, Myneni R B, Huang M, Zeng Z, Canadell J G, Ciais P, Sitch S, Friedlingstein P, Arneth A, Cao C, Cheng L, Kato E, Koven C, Li Y, Lian X, Liu Y, Liu R, Mao J, Pan Y, Peng S, Peñuelas J, Poulter B, Pugh T A M, Stocker B D, Viovy N, Wang X, Wang Y, Xiao Z, Yang H, Zaehle S, Zeng N (2016). Greening of the Earth and its drivers. Nat Clim Chang, 6(8): 791–795

Zhou M T, Li J, Zhu K W (2015). Changes of NDVI in different regions of northwest area and its responses to climate factor. Res. Soil Water Conserv, 22(3): 182–187

Zong L L, Wang R H (2014). Spatio-temporal changes of vegetation in Ningxia and its coupling relationship with climate factors. Sci Tech Engrg, 14(10): 153–159